Proceedings of the 4th Micro/Nanoscale Heat and Mass Transfer International Conference
MNHMT13
December 11-14, 2013, Hong Kong, China

MNHMT2013-22064

EXPERIMENTAL AND SIMULATION STUDY ON MOTION OF AN ISOLATED LIQUID PLUG INSIDE A DRY CIRCULAR CAPPILARY

Vyas Srinivasan
Doctoral Student
Department of Mechanical Engineering
Indian Institute of Technology Kanpur, India

Basant Singh Sikarwar
Project Scientist
Department of Mechanical Engineering
Indian Institute of Technology Kanpur, India

Sameer Khandekar
Associate Professor
Department of Mechanical Engineering
Indian Institute of Technology Kanpur, India

ABSTRACT

Classical study of motion of a single liquid plug (water) inside a micro/mini capillary tube is revisited to understand the contribution of meniscus friction and effect of contact angle hysteresis on the pressure required to initiate the motion of liquid plug of different *L/D* ratio. Experiments are carried out by injecting a known mass flow rate of air to push the liquid plug from rest. While the plug is at rest, as the air pressure increases linearly, the menisci deform till a limiting value, at which the plug starts moving. The initial phase of plug motion is dominated by its acceleration, which is then opposed by wall shear, and eventually leads to a steady motion of liquid plug at constant pressure and dynamic contact angle hysteresis.

Experimental results show that, the pressure required to initiate the motion of the liquid is independent of its length, indicating the dominance of static menisci friction at initial stages. Also, steady state pressure drop is observed to be much greater than that predicted by fully developed tube flow.

The flow is simulated in COMSOL using level set method. Simulation results agree well with the experimental result. Contribution of menisci towards static and dynamic friction and velocity development near menisci are obtained from simulations to model the friction factor for the flow.

Key Words: Menisci friction, Contact angle hysteresis, Static friction, Pressure drop

NOMENCLATURE

D	liquid plug diameter (m)
g	acceleration due to gravity (m/s^2)
L	liquid plug length (m)
ρ	density (kg/m^3)
p	pressure (N/m^2)
σ	surface tension (N/m)
t	time (s)
Δt	time step (s)
θ	static contact angle (degree)
θ_{adv}	contact angle at leading side of liquid plug at criticality of motion
θ_{rcd}	contact angle at trailing side of liquid plug at criticality of motion
$\Delta\theta$	contact angle hysteresis (θ_{adv} - θ_{rcd})
Δx	grid size in domain
$\dot{m}_{air}$	mass flow of air (kg/s)
α	volume fraction of liquid air (-)
κ	radius of curvature of liquid plug (m^{-1})
u_{fluid}	velocity of fluid (m/s)
u_i	velocity component in i^{th} direction (m/s)

INTRODUCTION

Micro-scale two-phase flow is an active area of research because of its varied applications in engineering devices, e.g., refrigeration, electronics cooling, catalyst coating in capillaries micro-reactors and porous media systems [1-3]. Taylor flow or capillary slug flow, characterized by long bubbles separated by liquid plugs, constitutes the typical regime under such conditions [4-7]. Many researchers [5, 8-13] have worked in the Taylor flow regime and tried to understand the thermo-hydrodynamic properties of such flows.

A review of local hydrodynamics of such flows, especially in the context of pulsating heat pipes, can be found in Khandekar et al. [14]. They reported that internal circulations

in liquid plug have been found to be the major cause of pressure drop. However, not many studies have reported the local meniscus level deformations, due to the imposed flow velocity and its subsequent impact on sensible transport phenomena of Taylor flows. Recently the motion of an isolated liquid plug in a long tube has also been reported [15-18]. These attempts have not been sufficient to explain the complex behavior of three phase contact line motion, contact angle hysteresis and other counter intuitive phenomenon. Present models available to predict the pressure drop and heat transfer in such flows, make considerable assumptions such as neglecting contact angle hysteresis, assuming no slip boundary conditions, etc., which leads to discrepancies in available understanding of physics. Also, most of the reported research emphasizes on the dynamic friction of liquid plug when at motion; the case of static friction of liquid plug in a mini/micro channel is less studied.

In this background, this paper is an attempt to understand the complex physics of motion of an isolated liquid plug inside a dry, circular, horizontal, glass capillary tube (of I.D. 1.5 mm). The experiment concentrates on the pressure required to initiate the motion of the liquid plug from rest to attainment of final steady-state velocity and the corresponding behavior of menisci deformation during the flow process. The role of contact angle hysteresis on pressure drop is also discussed.

The above phenomenon (liquid plug motion) is also simulated in COMSOL® for experimentally obtained data, such as static contact angle of liquid and contact angle hysteresis at criticality of motion of plug, at various *L/D* ratios in a circular capillary. Pressure variation and change of shape of liquid-air interface is captured during the simulation from rest to criticality of motion. Experimental and simulation data are in close agreement and show that the pressure required to initiate the motion of the liquid is independent of its length, indicating the dominance of menisci friction at initial stages. Also, the steady-state pressure drop is observed to be much greater than that predicted by classical tube flow friction factor.

EXPERIMENTAL STUDY

The experiment is carried out on a clean, dry, circular (I.D. 1.5 mm) glass capillary. Fig. 1 shows the schematic of the experimental set-up.

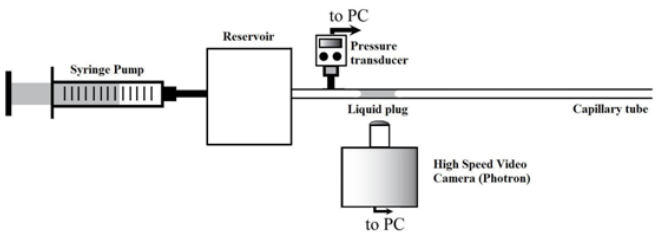

Fig. 1 Schematic of the experimental setup.

Known quantity of liquid (Water) is inserted carefully in the tube with a micro-syringe. Constant volume flow of air (25 ml/hr), fed from syringe pump is used to pressurize the liquid at rest till it overcomes the static friction and eventually attains a steady state velocity. The glass tube is thoroughly cleaned before each experiment. Time scale of experiment is much less than the time scale of evaporation of menisci. Also, the air injection from syringe pump is arranged so as to achieve quasi-constant volume air injection. The entire set-up is transparent to enable visualization of menisci (advancing and receding) deformation with high speed camera (Photron®) at 250 fps. The pressure data are collected using a sensitive pressure transducer (0-500 Pa, Huba Control®). Synchronization of high speed camera and pressure transducer is done to get accurate deformation behavior with time.

NUMERICAL SIMULATION

The COMSOL® commercial CFD software is used to model three-dimensional, transient, two-phase flow in micro-circular capillary. Fig. 2 shows a schematic of the circular micro capillary and the applied boundary conditions. The simulation is performed in two steps, as follows:

First step: static shape of water plug is determined by solving conservation of mass and momentum, together with an additional advection equation to determine the gas–liquid interface by applying the atmospheric pressure boundary condition at inlet and outlet, as shown in Fig. 2 (a).

Second step: by knowing the shape of interface face for given static contact angle, Equation (1-3) is solved for following boundary conditions: at inlet: the air flow with constant mass flow rate. The usual wetted boundary condition is applied at the wall and a zero normal pressure gradient boundary condition for all the variables is applied on the outlet. For an incompressible, Newtonian fluid, these equations can be written in tensor notation as follows:

Continuity equation:

$$\frac{\partial \rho}{\partial t} + \frac{\partial \rho u_j}{\partial x_j} = 0 \qquad (1)$$

Momentum equation:

$$\frac{\partial \rho u_i}{\partial t} + \frac{\partial \rho u_j u_i}{\partial x_j} = -\frac{\partial p}{\partial x_i} + \mu \frac{\partial u_i}{\partial^2 x_j} + F_s \qquad (2)$$

Volume fraction:

$$\frac{\partial \alpha}{\partial t} + u_i \frac{\partial \alpha}{\partial x_j} = \gamma \frac{\partial}{\partial x_j}\left(\varepsilon \frac{\partial \alpha}{\partial x_j} - \frac{\alpha(1-\alpha)\frac{\partial \alpha}{\partial x_j}}{|\frac{\partial \alpha}{\partial x_j}|} \right) \qquad (3)$$

where, i is free indices and j is repating indicies. u_i denotes the velocity vector in i^{th} direction , p the pressure, ρ the density and μ the dynamic viscosity of the fluid. F_s is the surface tension force approximated as a body force in th evicinity of the interface, and α is the volume fraction of one of the phases.The bulk properties, such as density and viscosity, are determined from the volume-fraction weighted average of the properties of the two fluids.

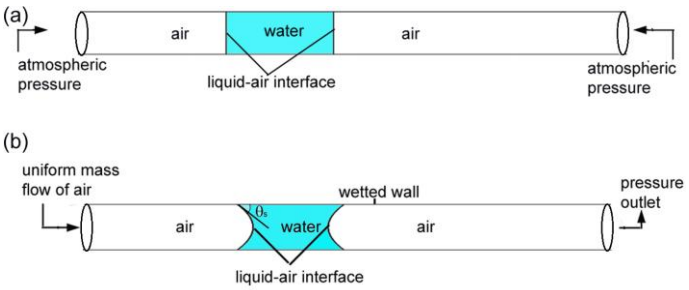

Fig. 2 Computational domain of circular capillary containing water and air. (a) Domain and corresponding boundaries for determined the static shape of plug for given static contact angle. (b) Domain and corresponding boundary conditions for determine the hydrodynamic behavior of liquid plug.

The detail of numerical methodology used in this paper is adopted from the COMSOL® multi-physics documentation [19]. The laminar two-phase flow level set method is used to identify the air–liquid interface by solving a volume fraction equation (Eq. (3) above) for one of the phases. An explicit geometric re-construction scheme is used to represent the interface by using a piecewise-linear approach. The time-step used for the VOF equation in COMSOL is not necessarily the same as that used for the other equations but is calculated based upon the characteristic transit time of a fluid element across a control volume and is limited by a specified maximum value for the Courant number (Co). The time taken to empty a cell is calculated by dividing the volume of each cell by the sum of the outgoing fluxes in the region near the fluid interface. The smallest such time is used as the characteristic time of transit for a fluid element across a control volume. The Courant number (Co) is defined by Eq. (4) as

$$Co = \frac{\Delta t}{\Delta x / u_{fluid}} \tag{4}$$

where, Δx is the grid size and u_{fluid} is the fluid velocity. A maximum Courant number of 0.025 is set in the present calculations and a variable time-step based on a fixed Courant number of 0.025 or less was used to force the time-step to be the same for all the equations.

Therefore, the terms on the left hand side (Equation 3) give the correct motion of the interface, while those on the right hand side are necessary for numerical stability. The parameter, which determines the thickness of the region where, goes smoothly from zero to one and is typically of the same order as the size of the element of the mesh. By default, it is constant within each domain and equals the largest value of the mesh size within the domain. The parameter determines the amount of re-initialization and stabilization of the level set function. It needs to be tuned for each specific problem. If it is too small, the thickness of the interface might not remain constant, and oscillation may appear because of numerical instabilities. On the other hand, if it is too large, the interface moves incorrectly. A suitable value is the maximum magnitude of the velocity field.

Table 1 Properties of the gas and the liquid used in the simulation

Fluid	ρ (kg/m^3)	μ (kg/ms)	σ (N/m)	θ_s (deg)	θ_{adv} (deg)	θ_{rcd} (deg)	$\dot{m}_{air}$ (kg/s)
Water	998	8.899 $\times 10^{-4}$	0.073	52	44	72	-
Air	1.175	1.751 $\times 10^{-4}$	-	-	-	-	8.16 $\times 10^{-9}$

The continuum surface force (CSF) model is used to model surface tension effects. The CSF model approximates the surface tension induced-stress by a body force, which acts throughout a small but finite fluid region surrounding the interface. The surface tension force per unit area is represented as:

$$F_s = \sigma \, \kappa \, \delta\left(r - r_{\text{int}}\right) n \tag{5}$$

where σ the coefficient of surface tension is, κ is the radius of curvature, n denotes the unit normal vector on the interface and $\delta(r)$ is the Dirac delta function, nonzero only at the fluid-air interface. The normal n and curvature κ in Eq.(5) are defined in terms of the volume fraction (α) via:

$$n = \frac{\nabla \alpha}{|\nabla \alpha|} \tag{6}$$

and

$$\kappa = \nabla n \tag{7}$$

the volume fraction (α) is also used to approximate the delta function by a smooth function defined by

$$\delta = 6\,|\alpha(1-\alpha)| \;\; |\nabla \alpha| \tag{8}$$

This implementation of the surface tension force can induce unphysical velocity near the interface known as spurious currents. This occurs because the pressure and viscous force terms do not exactly balance the surface tension force. The accurate calculation of gradients can help in minimizing these spurious currents.

In first step, a static contact angle of θ_s is specified in the wall of at initial condition. At the inlet and outlet boundary of capillary is defined as atmospheric pressure. In step second the shape of water plug is taken from the first step and solution is continue for input contact hysterics, constant air mass flow at inlet and constant pressure at outlet. Before start to find out the velocity field, water-air interfaces are deformed and acquire the shape according to the hysteresis.

A second order, non-iterative fractional step scheme is used for the time marching of the momentum and continuity equations. The correction tolerances for sub iterations (the ratio of the residual sat the current sub-iteration and the first sub-iteration) for pressure and momentum equations used are 0.01 and 0.001, respectively. The residual tolerance for both the equations was set to 1 e-06. The specified values of correction tolerances are much lower than the default values of 0.025 for the pressure equation and 0.0005 for the momentum equations.

The absolute values of residuals achieved were found to be sufficiently low $O(10^{-6})$ for velocities and $O(10^{-8})$ for continuity) using these correction and residual tolerances that the results were unaffected by the level of convergence achieved. A variable time step (Δt), based on a fixed Courant number of 0.025, and is used for the momentum and pressure equations.

RESULT AND DISCUSSION

An isolated liquid plug in equilibrium with atmosphere forms two distinct menisci. The static contact angle formed being governed by the Young's equation. As the air injection at constant volume flow rate (25 ml/h) starts, the pressure of the air pushing the liquid plug starts to increase linearly. While the liquid plug still at rest, due to the changing pressure, the two menisci deform, leading to contact angle hysteresis. Plug reaches criticality of motion when the air pressure force overcomes the reiteration due to the contact angle hysteresis.

Fig. 3 shows the pressure rise of pushing air and the corresponding deformation behavior of contact angle with time for different *L/D* ratio of liquid plug. For the given flow rate the drop reach the criticality at about the 17 second of commencement of experiment. At the criticality of motion the leading side angle of liquid plug is called as advancing angle and receding side contact angle is called receding angle and their value independent the *L/D* ratio of liquid plug, as shown in Fig. 3.

At this stage the plug is seen to move at constant pressure drop, greater the length of liquid plug, higher is the pressure drop, but is seen to be much higher than that predicted by classical Reynolds friction factor, this is attributed to the additional menisci friction and the contact angle hysteresis.

Fig. 4 shows the shape of plug at static condition captured during the simulation in circular capillary at various *L/D* ratios. It shows that the shape does not change with respect to *L/D*.

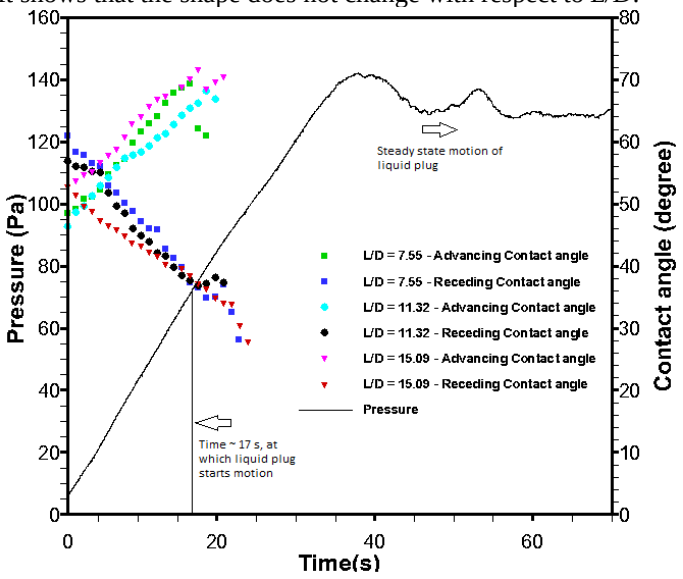

Fig. 3 Pressure curve and contact angle deformation when the plug is at rest.

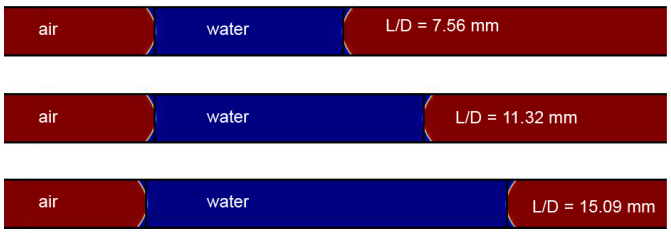

Fig. 4 Shape of liquid-air interface at various *L/D* ratios of water plug at static condition. Static contact angle is of 52°.

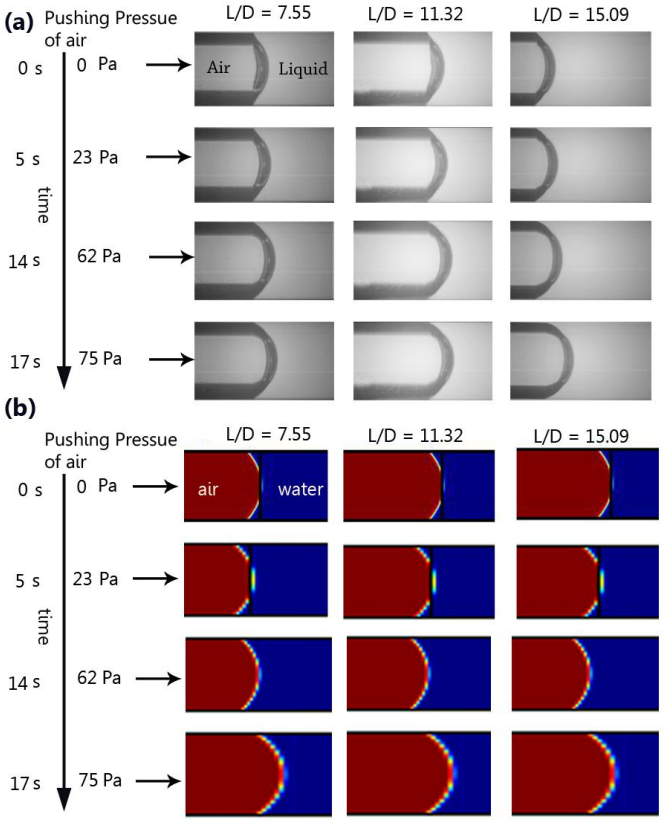

Fig. 5 Deformation of receding contact angle for different *L/D* ratio (a) experiment and, (b) simulation.

At this stage, static contact angle is of 52° and liquid air interface is equilibrium condition. There is no oscillation and fluctuation of the interface observed.

Fig. 5 shows the time evaluation of trailing side liquid-air interface of water plug from static equilibrium condition to criticality of motion observed during the experiment (Fig. 5(a)) and captured during the simulation (Fig. 5(b)). As the air injection at constant mass flow rate starts, it deformed. During the deformation, the trailing side contact angle decreases with time, as shown in Fig. 5(a-b).

Fig. 6 (a-b) shows advancing contact angle increases from the static contact angle. The deformation reaches a critical value, irrespective of the length of liquid plug, where the resistance of menisci is overcome and the liquid plug starts to move. The initial phase of plug motion is dominated by its

acceleration and the pressure continues to increase linearly, till a point where the opposing wall shear balances the pushing air force to reach a steady motion of liquid plug. At this stage the plug is seen to move at constant pressure drop, much higher than that predicted by classical Reynolds friction factor and the contact angle hysteresis remains same throughout.

Experimental and simulation result, as shown in Fig. 7 (a-b), clearly indicates that irrespective of the *L/D* ratio of liquid plug, the pressure at which the plug starts to move remains same. In addition, the deformation behavior of contact angle for different *L/D* ratio remains the same with time and pressure. This counter intuitive finding, strongly suggests that, the static friction is mainly due to the menisci friction. It is also seen the contact angle hysteresis for different *L/D* ratio of liquid plug is same at rest and the shape deformation of the liquid plug at rest is a function of pressure.

As the plug starts moving, the balance between pushing air pressure and dynamic wall shear balances out to reach a steady velocity. After attainment of this terminal velocity, the contact angle hysteresis remains the same through rest of its journey, till exit. This qualitatively explains the flow physics as seen from the experimental data. Fluctuations are observed on the pressure value, due to pinning of menisci on the glass surface.

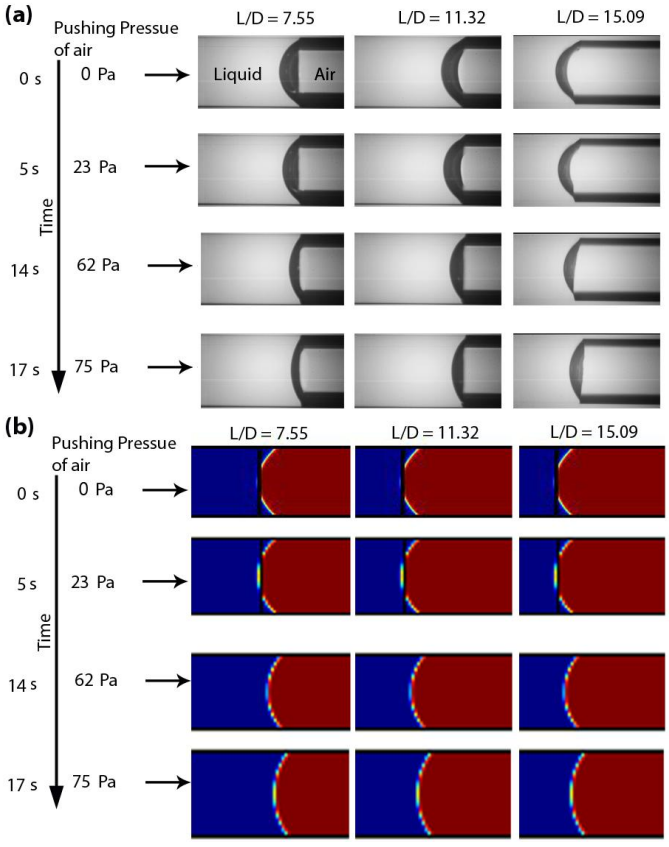

Fig. 6 Deformation of advancing contact angle for different *L/D* ratio (a) Shows experimentally observed meniscus shape and, (b) shows the corresponding values as observed by simulations.

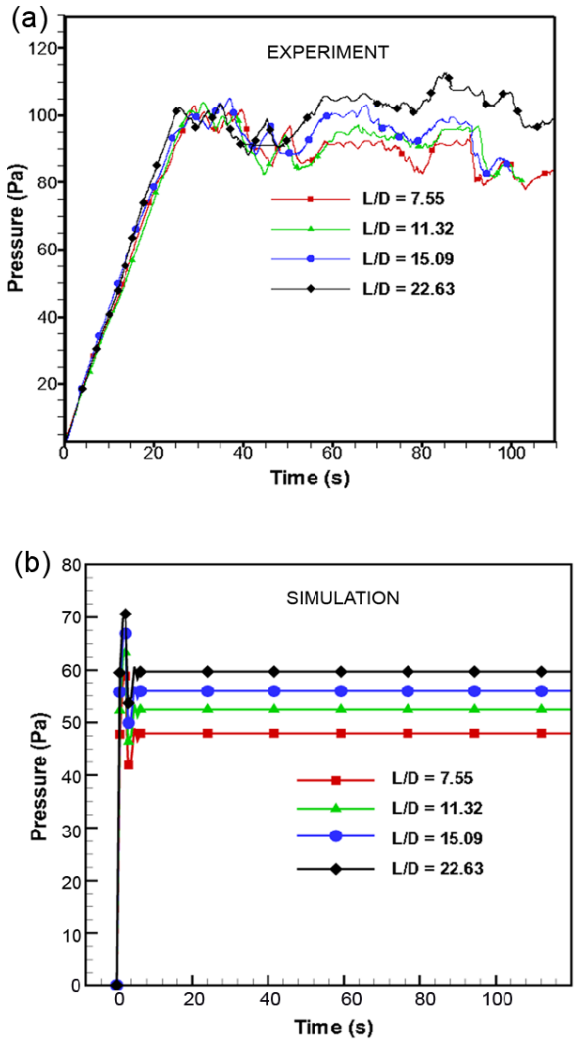

Fig. 7 Pressure vs time behavior for different length of liquid, starting from rest to attaining steady motion. (a) Experiment and (b) simulation.

SUMMARY AND CONCLUSIONS

Study of two-phase micro/mini channel flows (systems with Bo < 2) has had great impact in recent decade, right from micro-scale energy management to efficient drug delivery. Such flows have proved to be very efficient in active/passive thermal energy management such as electronic cooling, lab-on-chip, etc. Such flows involve complex contact line physics and are challenging from a modeling perspective. Understanding the local thermo-fluidic transport behavior has been a challenge due to several coupled and complex issues such as contact line dynamics, contact angle hysteresis, wettability, capillary instabilities etc. A concrete understanding of such flows is thus required, not only to understand the complete flow physics but also to make better efficient transport devices. In this background, experiment and simulations are carried out to understand the hydrodynamics of a single liquid (water) plug

inside a horizontal, dry, mini/micro circular tube (Bo < 2). A single liquid plug (of known *L/D* ratio) is pushed from rest by controlled injection of air, till attainment of quasi-steady terminal velocity. Visualization of liquid-air interface is done by using high speed camera for various *L/D* ratios. Simulation is carried out in COMSOL®, using level set method.

The significance of static and dynamic menisci friction and contact angle hysteresis in deciding the pressure required to initiate the plug motion is demonstrated. The results strongly indicate that the air pressure required for overcoming the static friction and initiate plug motion is independent of the length of the liquid plug, because of dominating surface forces. It is also observed that, while at rest, the advancing angle deforms more than the receding contact angle, till the pressure corresponding to static friction is reached. This hysteresis seems to be critical in deciding the static friction. Once the plug starts motion, the acceleration is opposed by wall shear, eventually leading to a steady terminal velocity, with constant pushing pressure and constant contact angle hysteresis. Simulation result fairly agrees with experimental observation. The source of discrepancy between experiment and simulation result is the assumption and approximation in the numerical model. Finding the contribution of menisci to friction and the velocity development at the interface are obtained from simulation to model a suitable relation between contact angle and friction coefficient.

ACKNOWLEDGEMENTS

Financial support from the Indo-French Centre for the Promotion of Advanced Research, New Delhi (Project #: 4408-1/2010), under the aegis of Indian Department of Science and Technology and the French Ministry of Foreign Affairs is gratefully acknowledged.

REFERENCES

[1] Gunther, A., Khan, S.A., Thalmann, M., Trachsel, F., and Jensen, K.F., 2004, "Transport and Reaction in Microscale Segmented Gas-Liquid Flow," *Lab on a Chip*, vol. 4, pp. 278–286.

[2] Kolb, W.B., and Cerro, R.L., 1991, "Coating the Inside of a Capillary of Square Cross Section, Chem. Engg. Sc.," vol. 46(9), pp. 2181–2195.

[3] Zheng, Y. Fujioka, H., and Grotberg, J.B., 2007, "Effect of Gravity, Inertia and Surfactant on Steady Plug Propagation in a Two-Dimensional Channel," Phy. Fluids, vol**.** 19, pp. 082107(1–66).

[4] Fairbrother, F., and Stubbs, A.E., 1935, "Studies in Electro-Endosmosis-1V.The Bubble Tube Method for Measurement", J. Chemical Society, vol. 1, pp. 527–529.

[5] Thulasidas, T.C., Abraham, M.A., and Cerro, R.L., 1997, "Flow Patterns in Liquid Slugs during Bubble-Train Flow Inside Capillaries", Chem. Engg. Science, vol. 52(17), pp. 2947–2962.

[6] Bretherton, F.P., 1961,"The Motion of Long Bubbles in Tubes", J. Fluid Mechanics, vol. 10, pp. 166–188.

[7] Taylor, G.I., 1961, "Deposition of a Viscous Fluid on the Wall of a Tube", J. Fluid Mechanics, vol. 10, pp. 161–165.

[8] Ghiaasiaan, S. M. and Abdel-Khalik, S. I., 2001, "Two-Phase Flow in Microchannels," Adv. Heat Transf., 34, 145–254.

[9] Cox, B.G., 1964, "An Experimental Investigation of the Streamlines in Viscous Fluid Expelled from a Tube", J. Fluid Mechanics, vol. 20, pp. 193–200.

[10] Oliver, D.R., and Wright, S.J., 1964, "Pressure Drop and Heat Transfer in Gas-Liquid Slug Flow in Horizontal Tubes", British Chemical Engineering, vol. 9, pp. 590–596.

[11] Chen, J.D., 1986, "Measuring the Film Thickness Surrounding a Bubble Inside a Capillary", J. Colloid Interface Science, vol. 109, pp. 341–349.

[12] Schwartz, L.W., Princen, H.M., and Kiss, A.D., 1986, "On the Motion of Bubbles in Capillary Tubes", J. Fluid Mechanics, vol. 172, pp. 259–275.

[13] Fermigier, M., and Jenffer, P., 1991, "An Experimental Investigation of the Dynamic Contact Angle in Liquid-Liquid Systems", J. Colloid Interface Science, vol. 146(1), pp. 226–241.

[14] Khandekar, S., Panigrahi, P.K., Lefevre, F., and Bonjour, J., 2010, "Local Hydrodynamics of Flow in a Pulsating Heat Pipe: a Review", Front. Heat Pipes, vol. 1, pp. 023003.

[15] Bajpai, A. K., Khandekar, S., 2013, "Thermal Transport Behavior of a Liquid Plug Moving Inside a Dry Capillary Tube", Heat Pipe Science and Technology, Accepted, DOI: 10.1615/HeatPipeScieTech.2013006563.

[16] Mehdizadeh, A., Sherif, S.A., and Lear, W.E., 2011, "Numerical Simulation of Thermofluid Characteristics of Two-phase Slug Flow in Microchannels", Int. J. Heat Mass Transfer, vol. 54, pp. 3457–3465.

[17] He, Q., Hasegawa, Y., and Kasagi, N., 2010, "Heat Transfer Modelling of Gas-Liquid Slug Flow without Phase Change in a Micro Tube", Int. J. Heat Fluid Flow, vol. 31, pp. 126–136.

[18] Gupta, R., Fletcher, D.F., and Haynes, B.S., 2009, "On the CFD Modelling of Taylor Flow in Microchannels", Chem. Engg. Sc., vol. 64, pp. 2941–2950.

[19] COMSOL® 4.2 multi-physics documentation, 2012.

